Linearized Active Circuits: Transfer Functions and Stability

Laurent Baratchart, Sylvain Chevillard, Adam Cooman, Martine Olivi, Fabien Seyfert

Linearized Active Circuits: Transfer Functions and Stability

Laurent Baratchart, Sylvain Chevillard, Adam Cooman, Martine Olivi, Fabien Seyfert

http://www.aimspress.com/journal/mine

Mathematics in Engineering, 4(5): 1–18.
DOI:10.3934/mine.2022039
Received: 13 July 2021
Accepted: 14 September 2021
Published: 12 October 2021

Research article

Linearized active circuits: transfer functions and stability

Laurent Baratchart[1], Sylvain Chevillard[1], Adam Cooman[2], Martine Olivi[1,*] and Fabien Seyfert[1]

[1] Factas, Inria, 2004 route des Lucioles, BP 93, 06902 Sophia Antipolis cedex, France

[2] Imec, Kapeldreef 75, 3001 Leuven, Belgium

* **Correspondence:** Email: martine.olivi@inria.fr; Tel: +33492387877; Fax: +33492387858.

Abstract: We study the properties of electronic circuits after linearization around a fixed operating point in the context of closed-loop stability analysis. When distributed elements, like transmission lines, are present in the circuit it is known that unstable circuits can be created without poles in the complex right half-plane. This undermines existing closed-loop stability analysis techniques that determine stability by looking for right half-plane poles. We observed that the problematic circuits rely on unrealistic elements with an infinite bandwidth. In this paper, we therefore define a class of realistic linearized components and show that a circuit composed of realistic elements is only unstable with poles in the complex right half-plane. Furthermore, we show that the amount of right half-plane poles in a realistic circuit is finite, even when distributed elements are present. In the second part of the paper, we provide examples of component models that are realistic and show that the class includes many existing models, including ones for passive devices, active devices and transmission lines.

Keywords: active circuits; transmission lines; linear time-delay systems; meromorphic transfer functions; stability analysis; Hardy spaces

1. Introduction

This work is motivated by the stability analysis of circuits containing active (non-linear) components, such as transistors and diodes, as well as distributed elements like transmission lines. A typical example is that of high-frequency amplifiers. The design of such devices relies today on powerful simulation tools in the frequency domain, like AC or S-parameter simulations [1]. These compute the circuit's response after it has been linearized around an equilibrium solution obtained via a DC simulation. The obtained equilibrium solution may either be stable, hence physically observable, or unstable, thus physically immaterial. Testing stability is thus mandatory before implementing the circuit. To this effect, a wide variety of methods has been proposed and we refer the reader to [2, 3] and their bibliography for a small sample of literature on the subject.

In this paper we focus on closed-loop local stability analysis. This approach, which requires little internal knowledge of the circuit, aroused considerable interest in the microwave community [3, 4]. The local stability is studied by computing the response of the circuit to small signal perturbations at its nodes, using AC analysis around a DC solution computed *via* a DC simulation. For instance, as shown in Figure 1, a small sinusoidal current source can input the circuit in parallel at a particular node k, and the voltage V_k at this node is taken as the output of the system. Then, a sweep of the frequency range is performed and the corresponding partial transfer function is estimated, pointwise in a bandwidth, as being the impedance seen by the current probe at the node under consideration.

$$G(s) = \frac{V_k(s)}{I_{\text{in}}(s)} \tag{1.1}$$

Determining the stability of $G(s)$ then allows to determine whether the equilibrium solution of the circuit is stable.

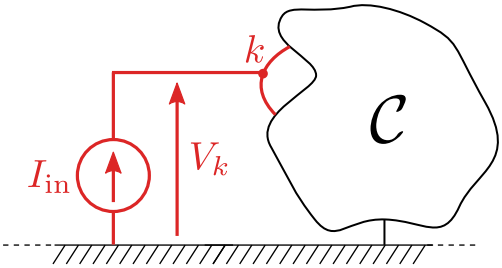

Figure 1. A partial transfer function of circuit C is determined by connecting a small-signal current source at node k and by determining the circuit's voltage response to this small-signal current excitation.

A standard definition of stability is: a linear stationary control system is stable when its transfer function belongs to $\mathcal{H}^\infty$, the space of bounded analytic functions in the open right half-plane. This is equivalent to require that the system maps inputs of finite energy (i.e., L^2 signals) to outputs of finite energy [5]. For a rational transfer function to be stable, it is necessary and sufficient that it has no pole in the closed right half-plane including at infinity. Such poles will be called unstable. Because partial frequency responses of circuits containing only lumped elements are rational, they are unstable if and only if they have at least one unstable pole. A common methodology in practice is to approximate the simulated frequency response of the linearized system by a rational function, the poles of which are used to assess the stability of the equilibrium [4]. Namely, the poles of a rational approximant are used to indicate the location of the poles of the true system, and poles lying in the closed right half-plane indicate instability.

It is natural to ask whether similar considerations apply to circuits with distributed elements. This is actually false. It is known there are quotients of quasi-polynomials, which typically represent transfer functions of delay systems, that are unstable though they have no unstable pole (these are neutral systems [6]). In [7] such a circuit was synthesized using resistors, inductors and capacitors, lossless transmission lines and negative resistances. The partial impedance presented by the circuit is

$$G(s) = \frac{2f(s)}{f(s) + 2} \tag{1.2}$$

where

$$f(s) = s\,\tanh(s) - \frac{1}{s+1}.$$

It can be shown that $G(s)$ has no poles in the closed right half-plane nor at infinity (where it has an essential singularity), and still it does not belong to $\mathcal{H}^\infty$.

At first, example (1.2) casts doubt on whether assessing the stability of an equilibrium, for active electronic devices, can be achieved upon checking if the linearized circuit has unstable poles. The components used to realize the example are however somewhat unrealistic, requiring lossless components and negative resistances with infinite bandwidth. In practice, no passive component is truly lossless and no active component has gain at all frequencies.

In this paper, we introduce a definition for realistic electronic components (Section 2), which become passive at infinite frequency (as opposed to ideal components). We study the stability of circuits composed of such realistic elements and show that instability without unstable pole can no longer happen: our main result is that a realistic circuit is unstable if and only if it has poles in the closed right half-plane. Moreover, these must be finite in number so that the unstable part of the linearized transfer function of a realistic circuit is demonstrably rational. In retrospect, this justifies to look for unstable poles thereof to check for stability at an operating point. Then, in Section 3, we discuss several component models which are realistic, to show that our definition applies to a broad class of models and that most common element models can easily be made realistic.

Hereafter, given a matrix M, we let M^t denote its transpose and M^* its conjugate transpose. The identity matrix is written $\mathbf{Id}$, irrespective of its size which will be understood from the context. The symbol $\Re$ is used to denote the real part.

2. Stability of linearized circuits under realistic assumption

We will work in the frequency domain to perform circuit analysis in this paper. We denote Laplace transforms with uppercase symbols, e.g., $V = V(s)$ is a function of a complex variable s which stands for the Laplace transform of the voltage $v = v(t)$ which is a function of the time t.

In the frequency domain, the behavior of a linearized component with n ports is described by an admittance matrix [8,9] of size n

$$\begin{bmatrix} I_1 \\ \vdots \\ I_n \end{bmatrix} = \begin{bmatrix} Y_{11} & \cdots & Y_{1n} \\ \vdots & \ddots & \vdots \\ Y_{n1} & \cdots & Y_{nn} \end{bmatrix} \begin{bmatrix} V_1 \\ \vdots \\ V_n \end{bmatrix} \tag{2.1}$$

where the voltages $V_1 \dots V_n$ are the node voltages with respect to the chosen reference node. The currents $I_1 \dots I_n$ are oriented so as to *enter* electronic components.

We adopt the paradigm that "what happens at very high frequencies is unimportant beyond passivity" and we set up a general definition of "realistic" that translates this requirement in mathematical terms for a large class of models.

Definition 1. *A linearized multiport is said to be Y-realistic if its admittance matrix Y is meromorphic on $\mathbb{C}$ and there exists $K > 0$ such that for any s satisfying $\Re(s) \geq 0$ and $|s| > K$:*
(i) $Y(s) + Y^*(s) \geq \alpha\,\mathbf{Id}$ for some $\alpha > 0$.[*]

[*] $A \geq B$ is in matrix sense, which means that $A - B$ is positive definite.

Similarly a linearized multiport is said to be Z-realistic if its impedance matrix $Z(s)$ is meromorphic on $\mathbb{C}$ and there exists $K' > 0$ such that for any s satisfying $\Re(s) \geq 0$ and $|s| > K'$:
(ii) $Z(s) + Z^*(s) \geq \beta\, \mathbf{Id}$ for some $\beta > 0$.
A multiport is said to be realistic if it is Z and Y-realistic.

In Section (3) we provide examples of realistic component models and show how to verify whether a given model satisfies the definition. In the remainder of this section we prove some important properties of the partial transfer functions $G(s)$ of circuits which comprise only realistic components. To that end, we compute the effect of I_{in} on the potential V_k using nodal analysis [9, sect.2.9]. We use nodal analysis because we are exciting the linearised circuit with a small-signal current source. When a small-signal voltage source is used to determine the partial transfer function of the circuit, a mesh analysis can be used to obtain similar results [9, sect.2.10]. When a combination of a voltage and current excitation is used, a modified nodal analysis or tableau method will be required to determine the partial transfer function, but this is outside of the scope of this paper.

To perform a nodal analysis we assign to each junction node j a potential V_j, and to each edge k an electric current I_k. One of the junction nodes, say V_n, is the ground (its potential is 0 by convention). *We always assume that the graph associated to the circuit is connected.* Specifically, we denote by $\mathbf{V} = (V_1, \ldots, V_{n-1})^t$ the vector of all node voltages (except V_n, the reference ground voltage) and by $\mathbf{I} = (I_1, \ldots, I_p)^t$ the vector of all currents in the branches. The *(node-branch) incidence matrix* of the circuit, say $\mathbf{A} = (A_{ij})$, has $n-1$ rows corresponding to the nodes (except the ground) and p columns corresponding the branches. It is defined by the rule:

$$\begin{cases} A_{ij} = 1 \text{ if edge } e_j \text{ is incident away from node } i, \\ A_{ij} = -1 \text{ if edge } e_j \text{ is incident towards node } i, \\ A_{ij} = 0 \text{ otherwise.} \end{cases}$$

Since the graph is connected, A has full row rank $(n-1)$ [10, Th. 2.1]. Kirchhoff's law gives us

$$\mathbf{A}\,\mathbf{I} = \mathbf{0} \tag{2.2}$$

Next, we substitute currents with voltages using relations (2.1). For this, we form the *branch admittance matrix*, a block diagonal matrix

$$\mathbf{Y}_b = \operatorname{diag}(Y_1, Y_2, \ldots, Y_h) \tag{2.3}$$

where the Y_j are the admittance matrices of the components in the circuit. With a convenient ordering of nodes and edges, it holds that $\mathbf{I} = \mathbf{Y}_b \mathbf{A}^t\, \mathbf{V}$, and (2.2) yields

$$\mathbf{Y}\,\mathbf{V} = \begin{pmatrix} 0 & \ldots & I_{\text{in}} & \ldots & 0 \end{pmatrix}^t, \tag{2.4}$$

where I_{in} is in position k and $\mathbf{Y}(s)$ is a $(n-1) \times (n-1)$ matrix, called *nodal admittance matrix*, which is related to the branch admittance matrix through ([9] Eq (2.9.8))

$$\mathbf{Y} = \mathbf{A}\mathbf{Y}_b\mathbf{A}^t. \tag{2.5}$$

The presence of ideal active components like diodes and transistors may result in $\mathbf{Y}$ being singular [7, 11] at all frequencies. Suppose that the Y_k are meromorphic functions on $\mathbb{C}$. As

meromorphic functions form a field [12, th. 15.12], the determinant of a matrix with meromorphic entries is again a meromorphic function. We call therefore *invertible as a meromorphic matrix*, any meromorphic square matrix with non zero meromorphic determinant. If the $Y_k's$ are supposed to be Y-realistic we will show in next proposition that $\mathbf{Y}$ in Eq (2.4) is invertible as a meromorphic matrix. By Cramer's rule, we then have:

$$V_j = (-1)^{k+j} \frac{\mathbf{Y}_{j,k}}{\det \mathbf{Y}} I_{\text{in}}. \tag{2.6}$$

where $\mathbf{Y}_{j,k}$ denotes the minor of $\mathbf{Y}$ obtained by deleting row j and column k. Thus, the voltage at node j depends linearly on I_{in} injected at node k, and the ratio V_j/I_{in} is the *partial transfer function* or *partial frequency response* of the circuit at node j from node k.

Proposition 1. *Assume that a linearized circuit made of Y-realistic components is excited at node k by a small current source as in Figure 1. Then,*

(i) The nodal admittance matrix $\mathbf{Y}(s)$ *of the linearized circuit (cf.* (2.5)*) is Y-realistic.*

and there exists $K > 0$ *such that, for any* s *satisfying* $\Re(s) \geq 0$ *and* $|s| \geq K$*, the following properties hold.*

(ii) $\mathbf{Y}$ *is invertible as a meromorphic matrix, therefore each partial frequency response* $Z_{k,j}(s)$ *of the circuit to the current source at node k is well-defined by* (2.6) *and meromorphic.*

(iii) Let $\|.\|$ *be the operator norm for matrices induced by the Euclidean norm on vectors. There exists* $M > 0$ *such that the matrix* $\mathbf{Z}(s) = \mathbf{Y}^{-1}(s)$ *verifies,*

$$\forall s \in \mathbb{C},\ \Re(s) \geq 0 \text{ and } |s| \geq K,\ \ \|\mathbf{Z}(s)\| \leq M.$$

Proof. (*i*) Each component i is Y-realistic and therefore meromorphic on $\mathbb{C}$, which causes $\mathbf{Y}_b$ to be meromorphic on $\mathbb{C}$. Meromorphic functions on a domain form a field of fractions, which makes $\mathbf{Y} = \mathbf{A}\mathbf{Y}_b\mathbf{A}^t$ meromorphic on $\mathbb{C}$.

According to Definition 1, the fact that component i is Y-realistic implies that there exists α_i such that $Y_i(s) + Y_i^*(s) \geq \alpha_i \mathbf{Id}$ whenever $\Re(s) \geq 0$ and $|s|$ is large enough. Let $\alpha_{\min} > 0$ be the infimum of the α_i. Then $\alpha_{\min} > 0$ and we have that the branch admittance matrix $\mathbf{Y}_b(s) + \mathbf{Y}_b^*(s) \geq \alpha_{\min}\mathbf{Id}$ for all s with $\Re(s) \geq 0$ and $|s| \geq K$, for some K.

Since the incident matrix $\mathbf{A}$ has full rank, by the assumed connectivity of the graph of the circuit, the symmetric matrix $\mathbf{A}\,\mathbf{A}^t$ is nonsingular so there exist $\lambda > 0$ such that $\mathbf{A}\,\mathbf{A}^t \geq \lambda\,\mathbf{Id}$. Letting $\alpha = \alpha_{\min}\,\lambda$, we deduce from (2.5) and the realness of $\mathbf{A}$ that assertion (*i*) holds.

(*ii*) Assume that for some s_0 satisfying $\Re(s_0) \geq 0$ and $|s_0| \geq K$, the matrix $\mathbf{Y}(s_0)$ fails to be invertible. Then, there is a non zero complex vector v such that $\mathbf{Y}(s_0)v = 0$, thus also $v^*\mathbf{Y}(s_0)v = 0$. Taking the real part, we get $v^*(\mathbf{Y}(s_0) + \mathbf{Y}^*(s_0))v = 0$ which contradicts the first item. The determinant of Y is therefore not the zero function, and assertion (*ii*) holds.

(*iii*) Combining assertion (*i*) with the fact that $\mathbf{Y} + \mathbf{Y}^* = \mathbf{Y}(\mathbf{Z} + \mathbf{Z}^*)\mathbf{Y}^*$, we have for $\Re(s) \geq 0$ and $|s| \geq K$ that

$$\mathbf{Z}(s) + \mathbf{Z}^*(s) \geq \alpha \mathbf{Z}(s)\,\mathbf{Z}^*(s)\,. \tag{2.7}$$

Letting $u(s)$ be a maximizing vector of $\mathbf{Z}^*(s)$ with unit norm, i.e., such that $\|Z^*(s)u(s)\| = \|Z(s)\|$, we get

$$\begin{aligned} 2\|\mathbf{Z}(s)\| &\geq u^*(s)\,(\mathbf{Z}(s) + \mathbf{Z}^*(s))\,u(s) \\ &\geq \alpha u^*(s)\,\mathbf{Z}(s)\,\mathbf{Z}^*(s)\,u(s) = \alpha\|\mathbf{Z}(s)\|^2, \end{aligned} \tag{2.8}$$

hence $\|\mathbf{Z}(s)\| \leq 2/\alpha$. □

We have proven that the branch admittance $\mathbf{Y}$ matrix of the circuit is Y-realistic. Working with the branch impedance matrix $\mathbf{Z}$ instead, it can be similarly proven that $\mathbf{Z}$ is Z-realistic. In fact, a linearized circuit made of active and passive realistic components is realistic in the sense of Definition 1. The dual of Proposition 1 can be proven, changing Z in Y and Y-realistic into Z-realistic.

Lemma 2. *Let $G(s)$ be a partial frequency response of a realistic linearized circuit. Then $G(s)$ is meromorphic on $\mathbb{C}$ and, for $|s| > K$ and $\Re(s) \geq 0$, $G(s)$ is bounded.*

Proof. The meromorphic property of G is a consequence of (*ii*) and its boundedness a consequence of (*iii*). □

Recall that $\mathcal{H}^\infty$ is the space of bounded analytic functions in the right half-plane Π^+. Recall also that a rational function is said to be strictly proper if it vanishes at infinity, i.e., if either the degree of the numerator is strictly less than the degree of the denominator or else it is the zero function.

Theorem 3. *Let $G(s)$ be a partial frequency response of a realistic linearized circuit. Then, $G(s)$ has only finitely many unstable poles. Specifically, there is a function $h \in \mathcal{H}^\infty$ and a strictly proper rational function $\mathfrak{r}$ having poles in the closed right half-plane only, such that $G(j\omega) = h(j\omega) + \mathfrak{r}(j\omega)$.*

Proof. Let $\overline{D(0,K)}$ denote the closed disk centered at 0 of radius K. By the previous lemma, the unstable poles of $G(s)$ (if any) lie in the compact set $\overline{\Pi}^+ \cap \overline{D(0,K)}$. Since $G(s)$ is a meromorphic function on $\mathbb{C}$, it can only have finitely many poles on a compact set. Hence $G(s)$ has at most finitely many unstable poles, as announced.

Number these unstable poles as $s_1 ... s_N$, with respective multiplicities $\nu_1, ... \nu_N$. Let $\mathfrak{r}_j = p_{\nu_j - 1}(s)/(s - s_j)^{\nu_j}$ be the principal part of $G(s)$ at s_j, where $p_{\nu_j-1}(s)$ is a polynomial of degree $\nu_j - 1$. It is a strictly proper rational function. Set $\mathfrak{r} = \sum_{j=1}^{N} \mathfrak{r}_j$; if $N = 0$ the sum is empty and we have that $\mathfrak{r} = 0$. By construction, $G - \mathfrak{r}$ is a meromorphic function with no poles in the closed right half-plane. Moreover it is bounded there for large $|s|$, because so is $G(s)$ by Lemma 2 and so is the strictly proper rational function $\mathfrak{r}$. Hence $G - \mathfrak{r} \in \mathcal{H}^\infty$, as was to be shown. □

In the notation of Theorem 3, checking stability of an equilibrium in a circuit to a small current perturbation at node k means finding out whether $\mathfrak{r} = 0$ or not for the partial frequency response $G(s)$ from node k. Determining whether a realistic circuit is stable therefore boils down to determining whether it has poles in the complex right half-plane. Of course, such a clear-cut answer is hard to make from simulations of $G(j\omega)$ at finitely many points of the imaginary axis.

The partial frequency response of a realistic circuit with distributed elements is expected to have an infinite amount of poles as is the case for most delay systems [5]. The speed of approximation by rational functions to transfer functions of delay systems is rather low [13–15], hence high order models are typically needed to reach good accuracy on a broad frequency interval. However, when the degree goes large, rational approximation techniques based on interpolation which are often favored by electronics engineers are known to generate spurious poles whose physical interpretation is uneasy [16, 17]; in fact, the extent to which the singularities of a rational approximant indicate those of the approximated function is a longstanding issue in approximation theory that cannot be answered independently of the approximation method one is using.

Theorem 3 suggests that identification methods should favor in this case a model class consisting of meromorphic functions with prescribed number n of poles in the right half-plane, because the theoretical response is of this type with $n = N$. This seems better suited than trying to fit a rational approximant with free poles to the non-rational function $G(s)$. Two approximation techniques appear to be of special interest in this connection. The first is the half-plane version of the Adamjan-Arov-Krein theory on meromorphic approximation with n poles in the uniform norm, also known as Hankel norm approximation, which is of standard use today in control and order reduction [18, 19]. The second is best meromorphic approximation with n unstable poles in L^2 of the line, which is equivalent to H^2-best rational approximation on the disk [20] for which efficient algorithms exist [21]. One would typically use this kind of approximation for increasing values of n: the case $n = 0$ gives an estimate of the size of the unstable part, while the case $n = N$ (of course N is unknown) would in principle allow one to recover $\mathfrak{r}$. Note that both algorithms work in the matrix-valued setting, which should be helpful to improve the estimation of $\mathfrak{r}$ by jointly approximating several partial frequency responses from the same node using a common denominator (*cf.* (2.6)) or even a block of partial frequency responses from a set of nodes to another set of nodes, using a matrix fractional representation for the block.

It is worth stressing that, at the functional level, computing $\mathfrak{r}$ is a linear operation. Assume indeed that the partial frequency response function $G(s)$ belongs to $L^2(j\mathbb{R})$, where $j\mathbb{R}$ denotes the imaginary axis. This is a realistic assumption in that it is fulfilled as soon as the response rolls off like $1/|\omega|$ at infinity, which is typical of capacitive effects. Then, $G(s)$ will be stable if and only if it belongs to the *Hardy space* $\mathcal{H}^2$ of the right half plane[†]. Similarly, let $\mathcal{H}^2_-$ denote the Hardy space of the left half-plane. Using the orthogonal decomposition

$$L^2(j\mathbb{R}) = \mathcal{H}^2 \oplus \mathcal{H}^2_-, \tag{2.9}$$

where $\oplus$ is the symbol for the direct sum of vector spaces, we see that the orthogonal projection of $Z(s)$ onto $\mathcal{H}^2_-$ is precisely $\mathfrak{r}$. In particular, the L^2-norm of the latter, as compared to the expected numerical error, provides one with an initial cheap test for instability [23, 24]. When the response is not square summable but merely bounded on the imaginary axis, similar considerations are still valid in a non Hilbertian context.

Of course several basic issues remain to be addressed in practice. First of all, one has to extrapolate finitely many pointwise data for $G(j\omega)$ on a limited range of frequencies into a function given at all frequencies. In this connection, the behavior at infinity is an important question that requires special care, for instance working with weights. This is essential to estimate the unstable part, which is not a trivial task. Also, one may have to study the quantitative behavior of the response in greater detail to decide how significant this unstable part is with respect to numerical errors. Such questions are left here for further research, but the fact that $G(j\omega)$ may in principle be computed with good precision at a great many frequencies, unlike in most identification problems, leads the authors to believe that the problem is indeed amenable to function-theoretic techniques.

3. Realistic models for components

We will now provide some examples of component models that are realistic. We start discussing passive components, where the key to being realistic is to have at least some losses. We also show that

[†]This space consists of holomorphic functions in the right half plane such that $\sup_{x>0} \|F(x + \,.)\|_{L^2(j\mathbb{R})} < \infty$ [22, Ch. 8].

lossy transmission lines are realistic. Finally, we discuss active components, like diodes and transistors.

3.1. Passive components

To rule out unrealistic behaviors of passive components, it is natural to select lossy multiports that involve perfect short or open circuits at no frequency. This is the object of the following definition which is compatible with the formalism developed in [25, Def. 2.1] :

Definition 2. *A passive multiport is said to be* very strictly passive *if its complex impedance matrix $Z(s)$ and its admittance $Y(s) = Z(s)^{-1}$ are meromorphic on $\mathbb{C}$ and satisfy, for $\Re(s) \geq 0$:*

(*i*) $Y(s) + Y^*(s) \geq \alpha\,\mathbf{Id}$ for some $\alpha > 0$,
(*ii*) $Z(s) + Z^*(s) \geq \beta\,\mathbf{Id}$ for some $\beta > 0$.

A very strictly passive multiport is clearly realistic. Condition (*ii*) is a frequency domain version of so-called *strict input passivity* of the system with transfer function Z, while (2.7) expresses its *strict output passivity*, see [26]. In the literature, a rational function satisfying (*i*) is called strongly strictly positive real [27, Def 2.54]. Note that the strict input passivity of the system with transfer function Z implies the strict output passivity of the system with transfer function Y. It should be noticed that, contrary to the rational case, meromorphic functions may have no limit at infinity.

3.1.1. Lumped passive components

Most passive components in a design, like resistors, capacitors, inductors and transformers, are modeled as an interconnection of several ideal lumped components. The obtained model is therefore a rational model and will be meromorphic on the whole complex plane.

It should be noted that this definition considers pure inductors and capacitors as unrealistic, since their impedance is unbounded on the imaginary axis. A realistic inductor can be obtained by connecting an ideal inductor in parallel with a large resistance R, and adding a small series resistance r as shown in Figure 2. We may think of R, e.g., as being the resistance of the air around the inductor, and of r as the resistance of the conductor constitutive of the element. Similar considerations apply to capacitors.

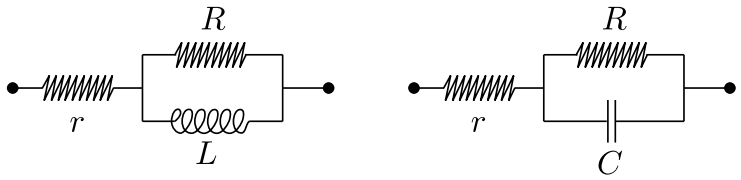

Figure 2. Realistic inductors and capacitors are lossy. A realistic capacitor or inductor model will therefore contain losses modeled as series and parallel resistors.

3.1.2. Transmission lines

We will now look into realistic models for transmission lines. They are passive components, so a realistic model should satisfy Definition 2. We start by constructing the Y-matrix of a transmission line and will then show that a lossy transmission line is indeed realistic.

Using the Telegrapher's equations, we describe the behavior of an infinitesimal piece of transmission line as a function of its per-unit-length parameters:

$$\begin{cases} -\frac{\partial V}{\partial x} = Z_l(s)\, I \\ -\frac{\partial I}{\partial x} = Y_l(s)\, V \end{cases} \tag{3.1}$$

where $Z_l(s)$ is the per-unit-length longitudinal impedance and $Y_l(s)$ is the per-unit-length transverse admittance [28]. For a transmission line with frequency-independent parameters, we have the following expressions for $Z_l(s)$ and $Y_l(s)$:

$$\begin{array}{rcl} Z_l(s) & = & sL + R \\ Y_l(s) & = & sC + G \end{array} \tag{3.2}$$

with $L, G, C, R \in \mathbb{R}^+$. In a lossless, frequency-independent line, $R = G = 0$. In general, $Z_l(s)$ and $Y_l(s)$ are more complicated strictly positive real functions which satisfy the Kronig-Kramers relations [28, 29]. We will discuss transmission lines with frequency-dependent parameters later.

From the per-unit-length properties of the line, the propagation constant $\gamma(s)$ and characteristic impedance $z_0(s)$ of the transmission line are defined as:

$$\gamma(s) = \sqrt{Z_l(s)\, Y_l(s)} \qquad \text{and} \qquad z_0(s) = \sqrt{\frac{Z_l(s)}{Y_l(s)}} \tag{3.3}$$

and the impedance matrix of a transmission line of length ℓ is then given by

$$Z(s) = \begin{bmatrix} z_0(s) \coth(\gamma(s)\,\ell) & \dfrac{z_0(s)}{\sinh(\gamma(s)\,\ell)} \\ \dfrac{z_0(s)}{\sinh(\gamma(s)\,\ell)} & z_0(s) \coth(\gamma(s)\,\ell) \end{bmatrix}. \tag{3.4}$$

To show that a transmission line model is realistic, we first have to show that it is meromorphic on $\mathbb{C}$. For a transmission line with frequency-independent parameters, the elements of the Z-matrix of the transmission line are meromorphic on the whole complex plane. Indeed, since $\gamma(s) = \sqrt{Z_l(s)\, Y_l(s)}$ is a function with a branchpoint of order 1 at each of its zeros, while cosh is entire and even, we see that $\cosh(\gamma(s)\,\ell)$ is an entire function. To show that $z_0^{-1} \sinh(\gamma(s)\,\ell)$ is meromorphic, we re-write it

$$\frac{\sinh(\gamma(s)\,\ell)}{z_0(s)} = \frac{\gamma(s)}{Z_l(s)} \sinh(\gamma(s)\,\ell)\,.$$

The sinh function is entire and odd. Therefore, $\gamma(s) \sinh(\gamma(s)\,\ell)$ is an entire function. Because $\cosh(\gamma(s)\,\ell)$, $\gamma(s) \sinh(\gamma(s)\,\ell)$ and $Z_l(s)$ are all meromorphic on the whole complex plane, we have that $z_0(s) \coth(\gamma(s)\,\ell)$ is meromorphic on the whole complex plane, which shows that the Z-matrix of a transmission line with frequency-independent parameters is meromorphic on the whole complex plane. In the appendix, we prove that a transmission line for which R, L, G, C are strictly positive is realistic.

3.2. Active devices

Active devices are modeled as a combination of a non-linear intrinsic device surrounded by a linear package, or extrinsic network [30, 31]. The extrinsic part of the model is a passive circuit, so the

package model should satisfy Definition 2 to be realistic. In this section, we discuss realistic intrinsic models for diodes and transistors.

The intrinsic part of a transistor is modeled as a lumped circuit. Distributed effects, like non-quasi-static behavior are commonly included using rational approximations [31, 32]. The linearisation of the intrinsic part will therefore result in a rational Y or Z matrix and is hence meromorphic everywhere on the complex plane.

3.2.1. Realistic diode models

The linearisation around an operating point for most diodes will result in a passive dipole, so a realistic model for such a diode should satisfy Definition 2. The linearisation of a tunnel diode, on the other hand, can exhibit a negative real part on the $j\omega$-axis for some operating points. A realistic tunnel diode cannot stay active for all frequencies, there should be a cutoff frequency where the dipole becomes passive: its complex impedance Z and complex admittance Y should satisfy the property that there is ω_c such that, whenever $|s| > \omega_c$ and $\Re(s) \geq 0$, then $\Re(Y(s)) \geq \alpha$ and $\Re(Z(s)) \geq \beta$, for some $\alpha, \beta > 0$. Both diode models proposed in Figure 3 satisfy this property, but many other, more complex models could also be used.

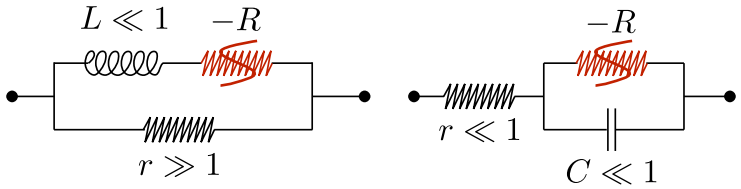

Figure 3. Two realistic models of a linearized diode. Left: With inductive effect and high resistance. Right: With capacitive effect and small resistance.

3.2.2. Realistic CMOS transistor model

Transistors can also be modeled in a realistic way, to account for the fact that actual devices have no gain anymore at very high frequencies. As an example on how to determine whether a given transistor model is realistic, consider the model for a linearised CMOS transistor in a common-source configuration as presented in Figure 4. We will show that this simple model only satisfies condition (i) of Definition 1. To do so, we start by determining the Y-matrix of the circuit. We obtain the following relation for the transistor without r_g:

$$\begin{bmatrix} I_G \\ I_D \end{bmatrix} = \underbrace{\begin{bmatrix} (C_g + C_{gd})s & -C_{gd}s \\ -C_{gd}s + g_m & C_{gd}s + g_d + C_d \end{bmatrix}}_{y(s)} \begin{bmatrix} U_i \\ V_D \end{bmatrix}.$$

In terms of $y(s)$, the admittance matrix of the complete circuit is expressed as:

$$Y(s) = \begin{bmatrix} \frac{y_{1,1}(s)}{1+r_g y_{1,1}(s)} & \frac{y_{1,2}(s)}{1+r_g y_{1,1}(s)} \\ y_{2,1}(s) - \frac{r_g y_{2,1}(s) y_{1,1}(s)}{1+r_g y_{1,1}(s)} & y_{2,2}(s) - \frac{r_g y_{2,1}(s) y_{1,2}(s)}{1+r_g y_{1,1}(s)} \end{bmatrix}$$

To determine whether $Y(s)$ is Y-realistic, we compute its asymptotic expansion at infinity

$$\begin{cases} Y_{1,1}(s) &= \frac{1}{r} + O(1/s) \\ Y_{2,1}(s) &= \frac{-C_{gd}}{r_g(C_{gd}+C_g)} + O(1/s) \\ Y_{1,2}(s) &= \frac{-C_{gd}}{r_g(C_{gd}+C_g)} + O(1/s) \\ Y_{2,2}(s) &= C_{gd}(1 - \frac{C_{gd}}{C_{gd}+C_g})s + 2g_d + 2g_m\frac{C_{gd}}{C_{gd}+C_g} + \frac{(C_{gd})^2}{r_g(C_{gd}+C_g)^2} + O(1/s) \end{cases} \tag{3.5}$$

Checking that the principal minors of the asymptotic expansion of $Y(s) + Y^*(s)$ deduced from (3.5) are bounded away from zero for $\Re(s) \geq 0$, yields that, under the assumption that $g_d > 0$, there exists ω_0 such that for $|s| > \omega_0$ and $\Re(s) \geq 0$ the matricial inequality $Y(s) + Y^*(s) \geq \gamma \mathbf{Id}$ holds for some $\gamma > 0$, which confirms that the model is Y-realistic. Note that this model could be rendered Z-realistic, and therefore completely realistic, by adding a resistor in series at the drain of the device.

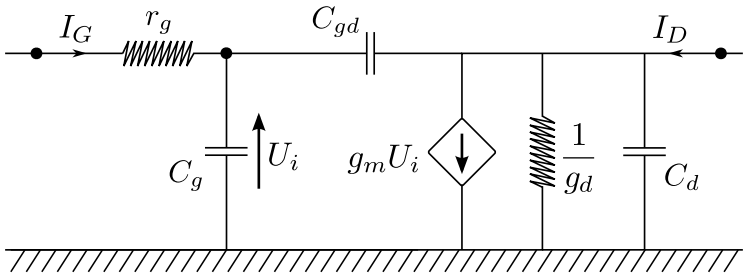

Figure 4. Y-realistic model of a linearized CMOS transistor in common-source configuration.

4. Illustrative example: a time-delayed Chua's circuit

The time-delayed Chua's circuit represented on Figure 5 is composed of a realistic model of a linearized diode (see Figure 3) and a block made of an ideal line with a resistor in series [33]. Using (3.4) with $\gamma(s)\ell = st$, where t is a time constant, the impedance of this block is computed as:

$$Z_{\text{lin}}(s) = Z_0 \frac{1 - ke^{-2st}}{1 + ke^{-2st}}, \text{with } k = \frac{Z_0 - R_S}{Z_0 + R_S} < 1.$$

Both the numerator and the denominator of $Z_{\text{lin}}(s)$ are quasi-polynomials of neutral type and since $|k| < 1$, it is easily checked that their roots lie on the vertical axis $\ln k/2t$. Thus, this block is realistic. This provides us with an alternative model of a realistic line: an ideal line in series with a resistor.

Since this linearized circuit is made of realistic components, by Proposition 1 and Lemma 2, the impedance $Z(s)$ measured at the red dot on Figure 5 is well-defined, meromorphic and for $\Re(s) \geq 0$, it is bounded outside a compact set. From Theorem 3, it has at most a finite number of unstable poles. Checking stability to small current perturbations at this node, amounts to determine whether $Z(s)$ has or not unstable poles. For this purpose, the method proposed in [23] and numerically implemented in [34], based on the stable/unstable decomposition (2.9), can be used. In the present example, $Z(j\omega)$ was determined on 1500 points between 0 and 9 GHz. The results are shown on Figure 6 and the circuit is clearly unstable. In addition, 4 poles in the right half-plane have been identified using the Principal

Hankel Components algorithm (PHC) [35]: two expected poles at 2 GHz and two positive real poles (at DC). Details can be found in the conference paper [24].

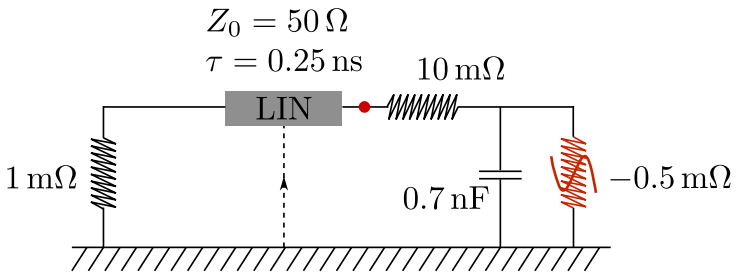

Figure 5. Time-delayed Chua's circuit made of realistic linearized electronic components.

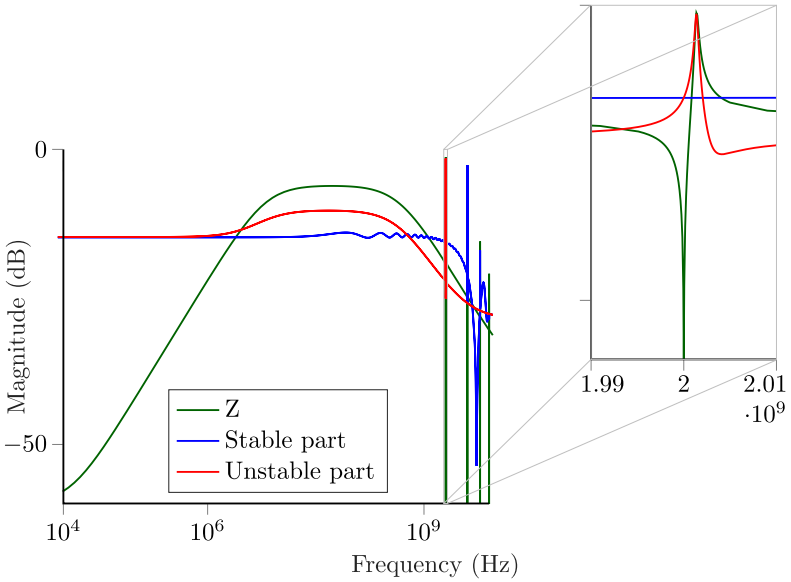

[H]

Figure 6. Stability analysis tractable: the impedance determined at the location of the red dot has a finite number of unstable poles.

Beyond the simplicity of this illustrative example, the method apply to any time-delayed system of this type, as soon as it is obtained from realistic linearized electronic components.

5. Generalization to lossy transmission lines with frequency-dependent parameters

So far, we only considered lossy transmission lines with frequency-independent parameters. However, many models of transmission line with frequency-dependent parameters can be found in the literature. In this section, we give the main ingredients to generalize Theorem 3 to the most common models encountered in the literature.

Such models may contain poles in $Y_l(s)$, associated with the time constant of a dielectric mechanism in the PCB material (see [28, 5.2] and [36]).

$$Y_l(s) = G + s\,\overline{\epsilon}(s)C \tag{5.1}$$

where G is the per-unit-length DC conductance, C is the per-unit-length static capacitance and $\overline{\epsilon}(s)$ is the normalized complex permittivity for the dielectric material. The poles of $\overline{\epsilon}(s)$ correspond to time-constants associated with relaxation of the dipoles in the dielectric and lie in the left half-plane. These models also take the skin effect into account. The latter is usually modeled by introducing terms in $\sqrt{s}$, thereby introducing a branch-point of order 1 in $s = 0$ in the expression for $Z_l(s)$:

$$Z_l(s) = R + sL + M\sqrt{s}f(\sqrt{s}), \tag{5.2}$$

where R, L, M are positive constants, and $f(u)$ is analytic with $\Re(f(u)) \geq 0$ on a neighborhood of $\{u : u = r\,e^{j\theta}, r \geq 0, -\pi/4 \leq \theta \leq \pi/4\}$, and asymptotic behavior at $u = \infty$ of the form (see [28])

$$f(u) = 1 + O(1/u).$$

The principal branch of $\sqrt{s}$ is used so that $Z_l(s)$ is strictly positive real on $\overline{\Pi}^+$. The branch-point at $s = 0$ in $Z_l(s)$ induces a branch-point at 0 in the Y and Z-matrices (3.4) of the transmission line. The poles as well as the zeros of $Y_l(s)$ and $Z_l(s)$ also give rise to branch-points for $Z(s)$ and $Y(s)$, but these lie in the open left half-plane. Thus, the Y and Z-matrices are meromorphic on a two-sheeted Riemann surface $\mathcal{S}_\epsilon$ above $\{s; \Re(s) \geq -\epsilon\}$, for some $\epsilon > 0$, with a branching of order 1 at 0.

Adapting the proofs of Theorem 5, Lemma 2 and Theorem 3 to the present case, where (3.2) gets replaced by (5.1) and (5.2), one can show the following results.

Firstly, properties (i) and (ii) of Definition 1 hold on the principal sheet. Secondly, if $G(s)$ is a partial frequency response of a realistic linearized circuit, including transmission line models with frequency dependent parameters as above, then it is meromorphic on a Riemann surface $S_{\tilde{\epsilon}}$ as above, for some $\tilde{\epsilon} > 0$ depending on the circuit. On the principal sheet, it has a Puiseux expansion at 0 of the form

$$G(s) = \sum_{l=-L}^{\infty} c_l\, s^{l/2}.$$

Let $\tilde{\Pi}_0^+$ (resp. $\tilde{\Pi}^+$) denote the subset of this sheet defined by $\Re(s) \geq 0$ (resp. $\Re(s) > 0$). Then, on the subset of $\tilde{\Pi}_0^+$ corresponding to $|s| > K$ for some $K > 0$, $G(s)$ is bounded. Consequently, on the imaginary axis viewed as a subset of $\tilde{\Pi}_0^+$, we have a decomposition

$$G(j\omega) = h(j\omega) + \sum_{l=-L}^{0} c_l\,(j\,\omega)^{l/2} + \mathfrak{r}(j\omega)\,, \tag{5.3}$$

where $h(s) \in \mathcal{H}^\infty$ and $\mathfrak{r}(s)$ is a strictly proper rational function having poles in the closed right half-plane only. Specifically, to get $h(s)$ we substract from $G(s)$ the singular part of the Puiseux expansion, and the singular part at the possible unstable poles which are finite in number, by the above mentioned generalization of Theorem 4. The resulting function $h(s)$ is analytic in $\tilde{\Pi}^+$ and bounded on compact subsets of $\tilde{\Pi}_0^+$. Finally, it is bounded on $\tilde{\Pi}_0^+$ because $G(s)$ is bounded for $|s| \geq K$ and so is the singular part there.

Equation (5.3) indicates that for circuits involving transmission lines with frequency varying parameters, some unstable singularity may occur at the zero frequency, which is of square root rather than polar type. Detecting this instability may be done systematically since it occurs at the known place $\omega = 0$, and if it is not present, then the stability analysis procedure described in Section 2 applies.

6. Conclusions

In this paper, we discussed properties of linear circuits containing lumped and distributed elements and their implications for closed-loop stability analysis. When the active devices in the circuit do not have finite bandwidth, it is possible to generate unstable circuits that have no poles in the right half-plane. We have therefore introduced a working definition for realistic components, based on the notion that realistic passive devices are not lossless and that active devices should become passive at very high frequencies. The main contribution of this paper is to show that a circuit made out of realistic components is unstable only when it has poles in the right half-plane. Moreover, a realistic circuit can have at most finitely many unstable poles, which makes its unstable part a rational function, even if distributed elements are present in the circuit.

To show that our definition of realistic components is feasible, we showed several examples of component models that are realistic, including passive devices, active devices and transmission lines.

Acknowlegdements

This research was funded in part by the CNES through grant R&T RS 10/TG1-019. We also wish to thank Juan-Mari Collantes, from Universidad del Païs Vasco/Euskal Herriko Unibertsitatea, for introducing the authors to electronic circuits and providing them with patient advice during long discussions on the subject.

Conflict of interest

The authors declare no conflict of interest.

References

1. K. S. Kundert, *The designer's guide to spice and spectre*, Kluwer Academic, 1995.
2. A. Suarez, R. Quere, *Stability analysis of nonlinear microwave circuits*, Artech House, 2002.
3. A. Suarez, Check the stability: Stability analysis methods for microwave circuits, *IEEE Microw. Mag.*, **16** (2015), 69–90.
4. J. Jugo, J. Portilla, A. Anakabe, A. Suarez, J. M. Collantes, Closed-loop stability analysis of microwave amplifiers, *Electron. Lett.*, **37** (2001), 226–228.
5. J. Partington, *Linear operators and linear systems*, London Math. Soc., 2004.
6. J. Partington, C. Bonnet, H_∞ and BIBO stabilization of delay systems of neutral type, *Syst. Control Lett.*, **52** (2004), 283–288.
7. L. Baratchart, S. Chevillard, F. Seyfert, On transfer functions realizable with active electronic components, INRIA Research Report RR-8659, 2014. Available from: `https://hal.inria.fr/hal-01098616`.
8. V. Belevitch. *Classical network theory*, Holden-Day, 1968.
9. H. Carlin, P. Civalleri, *Wideband circuit design*, CRC Press, 1998.

10. W.-K. Chen, *Applied graph theory*, North-Holland, 1971.

11. H. J. Carlin, D. C. Youla, Network synthesis with negative resistors, *Proceedings of the IRE*, **49** (1961), 907–920.

12. R. Walter, *Real and complex analysis*, Mc Graw-Hill, 1982.

13. P. M. Makila, J. R. Partington, Laguerre and Kautz shift approximation of delay systems, *Int. J. Control*, **72** (1999), 932–946.

14. M. G. Yoon, B. H. Lee, A new approximation method for time delay systems, *IEEE T. Automat. Contr.*, **42** (1997), 1008–1011.

15. L. Baratchart, S. Chevillard, Q. Tao, Minimax principle and lower bounds in h^2-rational approximation, *J. Approx. Theory*, **206** (2016), 17–47.

16. D. S. Lubinsky, Spurious poles in diagonal rational approximation, In: *Progress in approximation theory*, New York: Springer, 1992, 191–213.

17. L. D. Philipp, A. Mahmood, B. L. Philipp, An improved refinable rational approximation to the ideal time delay, *IEEE T. Circuits I*, **46** (1999), 637–640.

18. J. W. Helton, O. Merino, *Classical control using H^∞ methods: an introduction to design*, SIAM, 1998.

19. V. Peller, *Hankel operators and their applications*, Springer, 2003.

20. L. Baratchart, Rational and meromorphic approximation in L^p of the circle: system-theoretic motivations, critical points and error rates, In: *Computational methods and function theory*, World Scientific Publish. Co, 1999, 45–78.

21. M. Olivi, F. Seyfert, J.-P. Marmorat, Identification of microwave filters by analytic and rational H2 approximation, *Automatica*, **49** (2013), 317–325.

22. K. Hoffman, *Banach spaces of analytic functions*, Prentice-Hall, 1962.

23. A. Cooman, F. Seyfert, M. Olivi, S. Chevillard, L. Baratchart, Model-free closed-loop stability analysis: A linear functional approach, *IEEE T. Microw. Theory*, **66** (2018), 73–80.

24. A. Cooman, F. Seyfert, S. Amari, Estimating unstable poles in simulations of microwave circuits, In: *IEEE/MTT-S International Microwave Symposium - IMS*, 2018, 97–100.

25. R. Lozano, B. Maschke, B. Brogliato, O. Egeland, *Dissipative systems analysis and control: theory and applications*, Berlin, Heidelberg: Springer-Verlag, 2000.

26. N. Kottenstette, M. McCourt, M. Xia, V. Gupta, P. Antsaklis, On relationships among passivity, positive realness, and dissipativity in linear systems, *Automatica*, **50** (2014), 1003–1016.

27. B. Brogliato, R. Lozano, B. Maschke, O. Egeland, *Dissipative systems analysis and control*, Springer, 2007.

28. G. Miano, A. Maffucci, *Transmission lines and lumped circuits*, Academic Press, 2001.

29. J. S. Toll, Causality and the dispersion relation: logical foundations, *Phys. Rev.*, **104** (1956), 1760–1770.

30. G. Crupi, D. Schreurs, *Microwave de-embedding, from theory to applications*, Academic Press, 2014.

31. Y. Tsividis, *Operation and modeling of the MOS transistor*, Oxford University Press, 1999.

32. M. Bagheri, Y. Tsividis, A small signal dc-to-high-frequency nonquasistatic model for the four-terminal mosfet valid in all regions of operation, *IEEE T. Electron Dev.*, **32** (1985), 2383–2391.

33. M. Biey, F. Bonani, M. Gilli, I. Maio, Qualitative analysis of the dynamics of the time-delayed Chua's circuit, *IEEE T. Circuits I*, **44** (1997), 486–500.

34. A. Cooman, F. Seyfert, M. Olivi, Software Pisa. Available from: `https://project.inria.fr/pisa/examples/amplifier/`.

35. S. Y. Kung, K. S. Arun, Singular value decomposition algorithms for linear system approximation and spectrum estimation, In: *Advances in statistical signal processing*, JAJ Press, 1987, 203–250.

36. C. Gordon, T. Blazeck, R. Mittra, Time-domain simulation of multiconductor transmission lines with frequency-dependent losses, *IEEE T. Comput. Aid. D.*, **11** (1992), 1372–1387.

37. T. Ransford, *Potential theory in the complex plane*, Cambridge Univ. Press, 1995.

A. Proof that lossy transmission lines are realistic

In this appendix, we prove that lossy transmission lines with frequency independent parameters are realistic.

Lemma 4. *The impedance matrix $Z(s)$ and admittance matrix $Y(s)$ of a transmission line with positive real $Z_l(s)$ and $Y_l(s)$ are positive real.*

Proof. Let I_1 and I_2 be the currents entering each terminal of the transmission line and V_1 and V_2 be the potentials at each terminal. Let us write

$$\begin{aligned} P &:= V_1\,\bar{I}_1 + V_2\,\bar{I}_2 = V(0)\,\overline{I(0)} - V(\ell)\,\overline{I(\ell)} \\ &= -\int_0^\ell \left(\frac{\partial V}{\partial x}(\xi)\,\overline{I(\xi)} + V(\xi)\,\frac{\partial \bar{I}}{\partial x}(\xi)\right) \mathrm{d}\xi. \end{aligned}$$

Replacing $\partial V/\partial x$ and $\partial I/\partial x$ by their values in terms of I and V deduced from Equation 3.1, we obtain:

$$P = -\int_0^\ell \left(-Z_l(s)\;|I(\xi)|^2 - \overline{Y_l(s)}\,|V(\xi)|^2\right) \mathrm{d}\xi$$

therefore the real part of P, $\Re(P)$, is given by

$$\Re(P) = \int_0^\ell \Re\left\{Z_l(s)\right\}\;|I(\xi)|^2 + \Re\left\{Y_l(s)\right\}\;|V(\xi)|^2\,\mathrm{d}\xi. \tag{A.1}$$

Clearly the integrand is positive for $\Re(s) \geq 0$, hence $\Re(V_1\,\bar{I}_1 + V_2\,\bar{I}_2)$ is positive when $\Re(s) \geq 0$. This in turn implies that both $Y(s)$ and $Z(s)$ are positive real. □

Theorem 5. *A transmission line for which R, L, G, C are strictly positive is realistic.*

Proof. Let $Z(s)$ be the impedance of the line shown in (3.4) and set $\lambda = \max\{-R/L, -G/C\} < 0$. As $\gamma(s)$ and $z_0(s)$ are analytic and non-vanishing in the half-plane $\Pi_\lambda = \{s :\ \Re(s) > \lambda\}$, and since moreover

γ is never pure imaginary in Π_λ, the matrix Z is analytic there. As $\det(Z(s)) = z_0^2$, we get that $Y = Z^{-1}$ is likewise analytic. From (A.1) and the symmetry of Z, Y, we observe that $Z(s) + Z^*(s) = 2\Re(Z(s))$ and $Y(s) + Y^*(s) = 2\Re(Y(s))$ are positive symmetric matrices in Π_λ whose entries, being real parts of analytic functions, are harmonic functions of s. They are in fact positive definite at each $s \in \Pi_\lambda$, as (A.1) implies if $I_1 = x_1 + iy_1$ and $I_2 = x_2 + iy_2$ are not both zero that

$$\Re(P) = (x_1, x_2)\Re(Z(s))(x_1, x_2)^t + (y_1, y_2)\Re(Z(s))(y_1, y_2)^t > 0$$

(for in this case $\Re(Z_l(s)) > 0$ and $I(\xi)$ is not identically zero). We claim that

$$\Re(Y(j\omega)) \geq \alpha \mathbf{Id} \text{ for some } \alpha > 0, \tag{A.2}$$

and this will imply that (i) of Definition 2 is met. Indeed, if (A.2) holds and $u \in \mathbb{R}^2$ is a unit vector, the function $-u^t\Re(Y)u$ is a nonpositive harmonic function in Π_0 whose limit at every point of the imaginary axis exists and is at most $-\alpha$, therefore $-u^t\Re(Y)u$ is at most $-\alpha$ everywhere in Π_0 by the extended maximum principle [37, thm. 3.6.9]. To prove (A.2), we may restrict to large $|\omega|$ because on any compact interval of the imaginary axis it certainly holds by strict positivity of $\Re(Y(j\omega))$ and continuity of the latter with respect to ω. Without loss of generality, we choose the branch of the square root which is positive for positive arguments. In view of (3.4), we can write:

$$Y = z_0^{-1}\begin{bmatrix} \dfrac{1+e^{-2\gamma}}{1-e^{-2\gamma}} & -\dfrac{2e^{-\gamma}}{1-e^{-2\gamma}} \\ -\dfrac{2e^{-\gamma}}{1-e^{-2\gamma}} & \dfrac{1+e^{-2\gamma}}{1-e^{-2\gamma}} \end{bmatrix} = z_0^{-1}M. \tag{A.3}$$

Since $z_0(j\omega) \to \sqrt{L/C} > 0$ when $\omega \to \pm\infty$ and the matrix M in (A.3) is symmetric, it is enough to show that $M(j\omega)$ is bounded and that the eigenvalues of $\Re(M(j\omega))$ are greater than some $\delta > 0$ for $|\omega|$ large enough. Now, using the Taylor expansion of $(1+x)^{1/2}$ at $x \sim 0$, we get

$$\gamma(j\omega) = \sqrt{LC}\Big(j\omega + \frac{RC+GL}{2LC} + O(|\omega|^{-1})\Big)$$

so that $\Re(\gamma(j\omega)) \geq \kappa = \frac{RC+GL}{3\sqrt{LC}} > 0$, say, for $|\omega|$ large enough. Then $|e^{-2\gamma(j\omega)}| \leq e^{-\kappa} < 1$, hence $M(j\omega)$ is bounded. To prove that the eigenvalues of $\Re(M(j\omega))$ are greater than $\delta > 0$, we check that its trace and determinant are positive with $\det(\Re(M(j\omega))) \geq \eta > 0$ for $|\omega|$ large. Since the trace is bounded (recall $M(j\omega)$ is bounded), we will be done. First, it is readily seen that

$$\operatorname{tr}\Re(M(j\omega)) = 2\frac{1-e^{-4\Re(\gamma(j\omega))}}{|1-e^{-2\gamma}|^2}$$

is indeed positive. Next, a short computation yields that

$$\begin{aligned}\det(\Re(M(j\omega))) &= \frac{(1-e^{-4\Re(\gamma(j\omega))})^2}{|1-e^{-2\gamma}|^4} \\ &\quad -4\frac{(\Re(e^{-\gamma(j\omega)} - e^{-\gamma(j\omega)-2\bar\gamma(j\omega)}))^2}{|1-e^{-2\gamma}|^4} \\ &= \Big(1-e^{-4\Re(\gamma(j\omega))} + 2\cos(\Im\gamma(j\omega))e^{-\Re(\gamma(j\omega))}(1-e^{-2\Re(\gamma(j\omega))})\Big) \\ &\quad \times\Big(1-e^{-4\Re(\gamma(j\omega))} - 2\cos(\Im\gamma(j\omega))e^{-\Re(\gamma(j\omega))}(1-e^{-2\Re(\gamma(j\omega))})\Big) \\ &\quad \times|1-e^{-2\gamma}|^{-4}.\end{aligned}$$

So, we are left to prove that

$$1-e^{-4\Re(\gamma(j\omega))}\pm 2\cos(\Im\gamma(j\omega))e^{-\Re(\gamma(j\omega))}(1-e^{-2\Re(\gamma(j\omega))})$$

is positive and bounded away from 0 for $|\omega|$ large enough. As $0<e^{-\Re(\gamma(j\omega))}<e^{-\kappa}<1$, this comes from the fact that

$$1-2x+2x^3-x^4=(1-x)^3(1+x)$$

is strictly positive for $x\in(0,1)$. The same argument with z_0^{-1} replaced by z_0 in (A.3) gives us (*ii*) of Definition 2. □